Geophysical Research Letters

RESEARCH LETTER
10.1029/2022GL098132

Key Points:

- Elastic-net regularization can be used to automate covariate selection and reduce computational burden during trend surface development
- Additional physical covariates can improve trend surface results for certain regions

Supporting Information:

Supporting Information may be found in the online version of this article.

Correspondence to:

C. A. Love,
calove@uci.edu

Citation:

Love, C. A., Skahill, B. E., Russell, B. T., Baggett, J. S., & AghaKouchak, A. (2022). An effective trend surface fitting framework for spatial analysis of extreme events. *Geophysical Research Letters*, *49*, e2022GL098132. https://doi.org/10.1029/2022GL098132

Received 29 JAN 2022
Accepted 7 MAY 2022

An Effective Trend Surface Fitting Framework for Spatial Analysis of Extreme Events

Charlotte A. Love[1], Brian E. Skahill[2], Brook T. Russell[3], Jeffrey S. Baggett[4], and Amir AghaKouchak[5]

[1]Department of Civil and Environmental Engineering, University of California, Irvine, CA, USA, [2]US Army Corps of Engineers, Engineer Research and Development Center, Coastal and Hydraulics Laboratory, Portland, OR, USA, [3]School of Mathematical and Statistical Sciences, Clemson University, Clemson, SC, USA, [4]Department of Mathematics, University of Wisconsin—La Crosse, La Crosse, WI, USA, [5]Departments of Civil and Environmental Engineering and Earth System Science, University of California, Irvine, CA, USA

Abstract The estimation of exceedance probabilities for extreme climatic events is critical for infrastructure design and risk assessment. Climatic events occur over a greater space than they are measured with point-scale in situ gauges. In extreme value theory, the block maxima approach for spatial analysis of extremes depends on properly modeling the spatially varying Generalized Extreme Value marginal parameters (i.e., trend surfaces). Fitting these trend surfaces can be challenging since there are numerous spatial and temporal covariates that are potentially relevant for any given event type and region. Traditionally, covariate selection is based on assumptions regarding the topmost relevant drivers of the event. This work demonstrates the benefit of utilizing elastic-net regression to support automatic selection from a relatively large set of physically relevant covariates during trend surface estimation. The trend surfaces presented are based on 24-hr annual maximum precipitation for northeastern Colorado and the Texas-Louisiana Gulf Coast.

Plain Language Summary Extreme climatic events (e.g., extreme rainfall, wind) by their nature occur over a much larger space than they are measured with point-scale in situ gauges. Geographic and climatic variables (aka, covariates; e.g., elevation, temperature, pressure) that are associated with the extreme event type can be used to assist in properly modeling how the event varies over a given space. However, the selection of which geographic and climatic covariates should be included in spatial analysis of extremes is often left to manual selection and, in the case of extreme precipitation, is limited to only a few covariates (i.e., latitude, longitude, mean precipitation). Moreover, the use of a larger set of variables is often avoided due to the computational burden that is introduced. We demonstrate the use of elastic-net regularization for automating the selection of geographical and climatic covariates for modeling the distribution of extreme event parameters spatially, and for reducing the computational time needed for selecting the best performing set of covariates.

1. Introduction

The ability to estimate the magnitude and frequency of extreme atmospheric and hydrologic events is an essential part of infrastructure planning and hazard mitigation (Gumbel, 1958; Luke et al., 2017; Stedinger & Griffis, 2008). Given that many extreme events are spatial processes, model development has been focused on addressing the challenge of integrating spatial information within extreme value analysis methods (Cooley, 2009; Davison et al., 2012).

Block maxima approaches to spatial extreme value analysis borrow strength spatially, with the assumption that the distribution of the maxima at all locations in a region follow the generalized extreme value (GEV) family of distributions where some (or all) of its parameters vary spatially (i.e., trend surfaces) (Coles & Casson, 1998). Of these modeling approaches, the Regional Frequency Analysis (RFA) method is the industry standard for estimating the intensity, duration, and frequency of extreme events. The RFA method relies on geographic and climatological factors to assist in the delineation of subregions wherein the parameters of the underlying marginal distribution can be assumed to be acceptably homogeneous (Coles, 2001). However, marginal parameters are often spatially heterogenous. Therefore, Latent Variable Models (e.g., Bayesian Hierarchical Models) and Max-Stable Process approaches have been developed that allow for the integration of geographical and climatic covariates within

trend surfaces for distributing extremal model parameters in space (Banerjee et al., 2014; Cooley et al., 2007; Davison et al., 2012; Renard, 2011; Ribatet et al., 2012; Wikle et al., 1998).

A common challenge with utilizing these methods for spatial extreme value analysis is identifying the optimal set of spatial covariates (Blanchet & Davison, 2011; Davison et al., 2012; Ribatet, 2017). Poor trend surface characterizations can complicate the dependence parameterization since these models often make use of a log-likelihood formulation (Blanchet & Davison, 2011; Ribatet, 2017). For example, when working with a max-stable process model that uses a pairwise log-likelihood, there are 2^n possible models that involve subsets of n predictors (James et al., 2013). If $n = 10, 100$, then there are 1,024, $1.267651e^{30}$ possible models to be considered for a single marginal parameter trend surface. Therefore, we introduce the addition of elastic-net regularization during trend surface development to automate covariate selection and to reduce the computation time needed for the log-likelihood stage of spatial model development. While the methods in this study focus on using the GEV family of distributions based on a block maxima approach (e.g., annual maxima), these improvements to trend surface modeling can be applied to models that utilize other distributions.

2. Methods

For spatial models of extremes, we often use covariate information from each site across the region to model the spatially varying GEV parameters (i.e., trend surfaces). The spatially varying GEV parameters are determined using the at-site extreme value distribution fit of the AM data. The linear trend surfaces used within latent variable and max-stable process approaches are commonly of the form

$$\begin{aligned}\mu(\mathbf{cov}_\mu) &= \eta_{\mu,0} + \eta_{\mu,1} cov_{\mu,1} + \cdots + \eta_{\mu,n_\mu} cov_{\mu,n_\mu}\\ \sigma(\mathbf{cov}_\sigma) &= \eta_{\sigma,0} + \eta_{\sigma,1} cov_{\sigma,1} + \cdots + \eta_{\sigma,n_\sigma} cov_{\sigma,n_\sigma}\\ \xi(\mathbf{cov}_\xi) &= \eta_{\xi,0} + \eta_{\xi,1} cov_{\xi,1} + \cdots + \eta_{\xi,n_\xi} cov_{\xi,n_\xi}\end{aligned} \tag{1}$$

where $\eta_{\cdot,i}$, $cov_{\cdot,i}$, and n_μ, n_σ, n_ξ are the parameters, site-specific covariates, and the number of non-zero covariates for the GEV distribution's location (μ), scale (σ), and shape (ξ) parameters that are derived from univariate at-site estimates. Using either Bayesian methods or a maximum likelihood approach we can then find the best set of parameters (i.e., intercept and regression coefficients) indicated in Equation 1 that minimize the error between the at-site GEV parameter fits and the model containing the covariates.

Our proposed process for trend surface model selection involves two stages. First, elastic-net regularization is run using k-fold cross validation to select the best fitting general linear models for each GEV parameter independently (Equation 1). For the second step, a sampling of the best fitting models for each parameter are selected based on the elastic-net results and then run in combination within a spatial GEV framework (latent process model) to determine the best trend surface for the region.

Elastic-net regularization is a hybrid of ridge and lasso regression that makes use of the strengths of each method, while minimizing their shortfalls (Friedman et al., 2010). Ridge regression is known for yielding smooth solutions that keep all the predictors, which makes it good in the case of correlated variables but not ideal if parsimony is desired. Whereas lasso regression results in automatic variable selection that does not handle correlated variables well but it does tend to select the most sparse solutions (James et al., 2013). The elastic-net penalty was originally introduced by Zou and Hastie (2005) as a compromise between ridge (Hoerl & Kennard, 1970; Tikhonov, 1943) and lasso (Tibshirani, 1996) regression. Given observations y_i, $i = 1, \ldots, n$, an $n \times m$ matrix of normalized covariates $\mathbf{X}$ and an assumed linear model

$$y_i = \eta_0 + \eta_1 x_{i,1} + \cdots + \eta_m x_{i,m}, \tag{2}$$

the elastic net minimizes

$$\frac{1}{2n}\sum_{i=1}^{n}\left(y_i - \eta_0 - \eta x_i^T\right)^2 + \lambda\sum_{j=1}^{m}\left[\frac{1}{2}(1-\alpha)\eta_j^2 + \alpha|\eta_j|\right], \tag{3}$$

where λ is a non-negative regularization parameter that is tuned to weight the overall strength of the penalty and $\alpha \in [0, 1]$ is specified to control the penalty term to vary from ridge regression at $\alpha = 0$ to lasso regression at $\alpha = 1$ (Friedman et al., 2010). As α increases from 0 to 1 for a fixed λ, the number of zero-valued η_j increases from 0 to the sparsity of the lasso (Friedman et al., 2010). In this study, variable selection was desired in the interest of adherence with the principle of parsimony, therefore α was specified close to 1 for numerical stability (Friedman et al., 2010). With α specified close to 1, the elastic net performs much like lasso regression while retaining ridge regression's capacity to collectively shrink the coefficients for any highly correlated covariables (Friedman et al., 2010; Hastie et al., 2009). Exploiting extreme value theory, each independent elastic-net application used univariate at-site GEV estimates as the observations. Employing the "glmnet" R package (Simon et al., 2011), repeated k-fold cross-validation (CV) was used to find the minimizing value for λ (Equation 3) for each elastic-net application (Equation 2). The minimizing model ($\lambda_{\min}$) is the one with the lowest CV mean squared error (MSE), while the best regularizing model λ_{reg} is defined as having the largest λ value within one standard error of $\lambda_{\min}$ (Friedman et al., 2010; Hastie et al., 2009, 2016).

For the second step of the trend surface modeling, spatial GEV models were fitted and evaluated using the "SpatialExtremes" R package, which uses a maximum likelihood approach (Ribatet, 2020). A sampling of the best performing trend surfaces (e.g., top 10) from the elastic-net CV for $\mu(\mathbf{cov}_{\mu})$, $\sigma(\mathbf{cov}_{\sigma})$, and $\xi(\mathbf{cov}_{\xi})$ from the range $[\lambda_{\min}, \lambda_{reg}] \cup (\lambda_{reg}, \lambda_{\max})$, where $\lambda_{\max}$ corresponds with the intercept only model, were selected and simultaneously fitted. For example, if there were 10 top models for each GEV parameter and an intercept only model for each, then there would be $11^3 = 1{,}331$ spatial GEV models to be fitted. The log-likelihood of the spatial GEV model used is given by

$$l(\eta_{\mu}, \eta_{\sigma}, \eta_{\xi}) = \sum_{i=1}^{n_{site}} \sum_{j=1}^{n_{obs}} \left\{ -\log\sigma_i - \left(1 + \xi_i \frac{y_{i,j} - \mu_i}{\sigma_i}\right)^{\frac{-1}{\xi_i}} - \left(1 + \frac{1}{\xi_i}\right) \log\left(1 + \xi_i \frac{y_{i,j} - \mu_i}{\sigma_i}\right) \right\}, \quad (4)$$

where μ_i, σ_i, and ξ_i are the GEV parameters for the ith site ($i = 1, \ldots, n_{site}$) with ξ_i assumed non-zero, and $y_{i,j}$ is the jth observation for the ith site (Ribatet, 2009). The spatial GEV models were evaluated using information criterion scores (i.e., Takeuchi Information Criterion) (Takeuchi, 1976) and quantile-quantile comparisons of the spatial GEV model parameter estimates with their at-site counterparts (Blanchet & Davison, 2011; Ribatet, 2009).

3. Data

Two regions with distinct geographic and climatic drivers for the dominant storms observed within each region were selected for study (Figure 1). These regions include northeastern Colorado (NECO) and the Texas-Louisiana (TXLA) Gulf Coast. The Front Range region of Colorado is dominated by localized thunderstorms during the summer months, while the Gulf Coast region is dominated by tropical cyclones (Schumacher & Johnson, 2006; Shepherd et al., 2007). Observed daily precipitation data was retrieved from the NOAA Global Historical Climatology Network-Daily (GHCN-Daily) data set (Menne, Durre, Korzeniewski, et al., 2012; Menne, Durre, Vose, et al., 2012) for both NECO and TXLA. The 24-hr duration annual maxima (AM) time series were produced using gauged sites with at least 40 years of data available with no more than 10% missing data in any given year. The precipitation time series at these gauged sites were also checked for stationarity over the period of 1960–2020 using a Mann-Kendall trend test with an α of 0.05.

The covariate data selected includes longitude, latitude, their product, elevation, and relevant annual and monthly climatological information (i.e., precipitation, dewpoint temperature, maximum/minimum/mean temperature, and maximum and minimum vapor pressure deficit) extracted from the Parameter-elevation Relationships on Independent Slopes Model (PRISM) Norm81 m long-term (1981–2010) mean monthly gridded data sets at 30 arc second resolution (Daly et al., 2008) for all gauged sites within both study regions. These covariates and their squares constituted the entire set of covariables (190 in total) considered to build each trend surface within both study regions. The selection of these covariates was based on past literature that demonstrates the links between local extreme precipitation, physical information (e.g., elevation, climatology) (Javier et al., 2007; Oki et al., 1991; Papalexiou et al., 2018), and rainfall-temperature thermodynamic relationships (Adler et al., 2008; Trenberth & Shea, 2005; Zhao & Khalil, 1993).

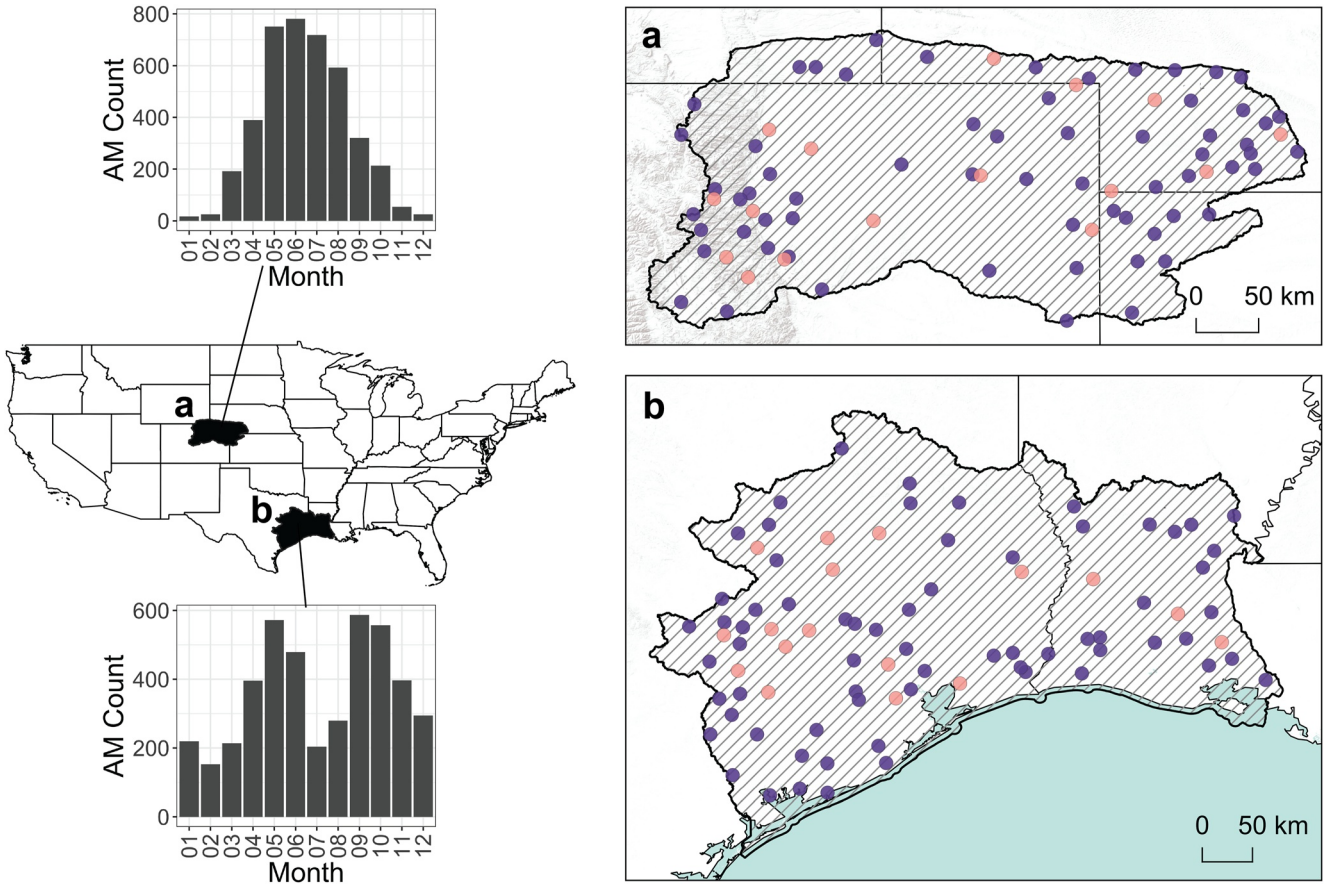

Figure 1. Study regions and sites associated with the observed annual maxima data. The regions are (a) northeastern Colorado and (b) the Texas-Louisiana Gulf Coast. Purple markers indicate calibration sites, while orange markers indicate validation sites. Annual maxima counts by month are also displayed for each region.

4. Results

Each respective elastic-net application was performed using 20 separate iterations of k-fold CV for each GEV parameter with a k of 10 and an α of 0.95 for both regions. Figure 1 shows the gauged sites for both regions that were randomly selected for the 80% calibration (purple markers) and 20% validation (orange markers) AM data sets. An α of 0.95 was selected to achieve an α value that would favor the parsimonious lasso regression, while still incorporating ridge regression's ability to reduce the coefficients for any highly correlated covariables (Friedman et al., 2010). After narrowing down the results to the best performing k-fold CV run out of the 20 iterations, a sampling of the general linear models within that run was made over [$\lambda_{\min}$, λ_{reg}] along with the intercept. Instead of simply selecting the best minimizing model $\lambda_{\min}$, we chose to test multiple models within this range since several performed relatively well (e.g., Figure 2a). The results for each region's parameters are displayed in Figure 2 with the $\lambda_{\min}$ and λ_{reg} models indicated by dashed vertical lines.

In the second step of the trend surface modeling, the goal is to test all possible combinations of the sampled location, scale, and shape models to find the best single combined set within a spatial GEV framework. Table 1 details the non-zero covariates of the spatial GEV models with the lowest Takeuchi Information Criterion (TIC) by region that were selected from this iterative process. The QQ-plots for the best of the top models for each regions' trend surfaces can be seen in Figure 3, which compare the fit of the observed with our model results. The modeled location and scale parameters fit relatively well at both the calibration and validation sites (Figure 3, columns 1–2).

While the standard practice for the shape parameter is to set it to a fixed value, the variability in the shape parameter indicates that this would not be the best option given the data within these regions (Figure 3, far right column). Of particular interest is that the increased number of covariates for the TXLA's model achieved an improved fit

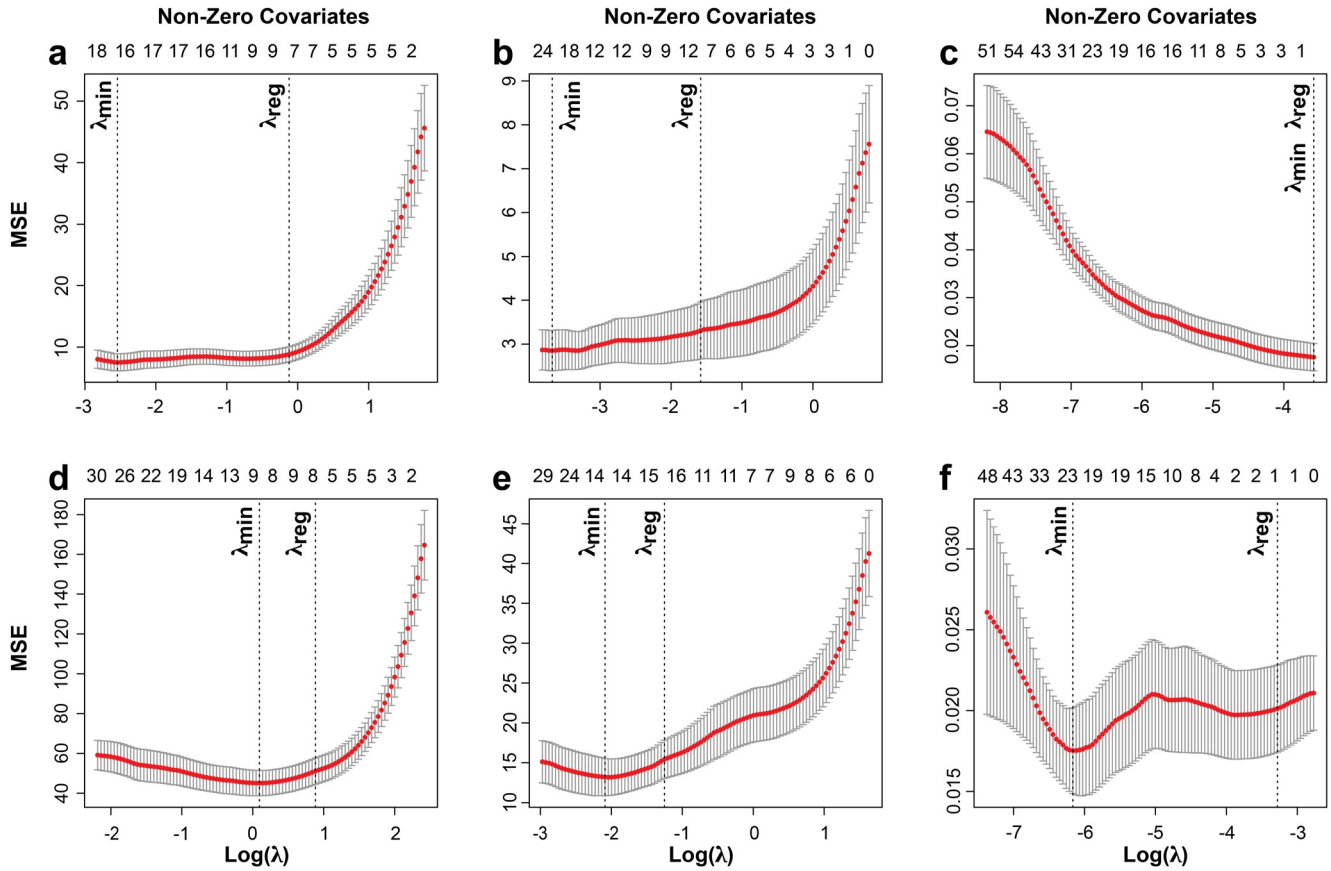

Figure 2. Elastic-net cross-validation (CV) summary plots for the northeastern Colorado (top row) and Texas-Louisiana (bottom row) that demonstrate the results for (a and d) $\mu(\mathbf{cov}_{\mu})$, (b and e) $\sigma(\mathbf{cov}_{\sigma})$, and (c and f) $\xi(\mathbf{cov}_{\xi})$. The x-axis is the natural logarithm of λ, the y-axis is the mean squared error (MSE), the top of the plot indicates the number of non-zero covariates as λ varies, the red markers are the CV derived MSE with error bars indicating one standard error, and the dotted vertical lines indicate the locations of the CV identified λ-value that minimizes the MSE ($\lambda_{\min}$) and the defined best regularizing model (λ_{reg}).

of the shape parameter's spatial variability without compromising the model's performance at the validation sites (Figure 3f). Had we not introduced the elastic-net regularization step within our trend surface modeling, we likely would not have chosen to use those covariates and would have settled for a worse fitting trend surface unknowingly. We found that using the same covariates for both the location and scale parameters as were used for the top model and setting the shape parameter to a constant value (no covariates) results in worse model performance for

Table 1
The Non-Zero Covariates and the Signs of Their Coefficients for Each Region's Selected Trend Surface Models[a]

	$\mu(\text{cov}_{\mu})$	$\sigma(\text{cov}_{\sigma})$	$\xi(\text{cov}_{\xi})$
NECO	$-X, +Y, +P_{Mar}, -P_{May}, +P_{Jun}, -P_{Oct}, +P^2_{May}, +P^2_{Jul}, +P^2_{Aug}, -P^2_{Dec}, +T_{D,Apr}, +T_{D,May}, +Min.T^2_{Oct}, +Max.VPD_{Jul}, -Min.VPD_{Jun}, +Max.VPD^2_{Jul}, +Min.VPD^2_{Mar}, +Min.VPD^2_{Nov}$	$+Z, +P_{Mar}, -P^2_{May}, +P^2_{Jul}, -P^2_{Dec}, +T_{D,Nov}, -MeanT^2_{Mar}, +Min.VPD^2_{May}, +Min.VPD^2_{Oct}, +Max.VPD_{Aug}, +Min.VPD^2_{Mar}, -Min.VPD^2_{Dec}$	$-MeanT^2_{Mar}, +Min.VPD_{Dec}$
TXLA	$-Z, +P_{May}, +P_{Jul}, +P^2_{Jan}, +P^2_{Oct}, +T_{D,Jan}, -MeanT_{Jul}, -Min.VPD_{Jan}, +Max.VPD^2_{Jul}, -Max.VPD^2_{Sep}, +Min.VPD^2_{Jun}, +Min.VPD^2_{Jul}$	$+Z, +P_{Sep}, +P_{Nov}, +P^2_{May}, +P^2_{Oct}, +T_{D,Jul}, -T^2_{D,Dec}, +Max.T^2_{Jan}, +Max.T^2_{Dec}, +Min.VPD^2_{Jul}$	$+Z, -P^2_{Apr}, +P^2_{Oct}, -MeanT_{Aug}, +MeanT^2_{Aug}, +Max.T^2_{Jun}, -Max.VPD_{Dec}, -Min.VPD_{Mar}, +Min.VPD_{May}, -Min.VPD_{Jul}$

Note. NECO, northeastern Colorado; TXLA, Texas-Louisiana.

[a]Covariates *X*, *Y*, *Z* are longitude, latitude, and elevation, respectively. Covariates in the table also include monthly precipitation (*P*), monthly mean, maximum, and minimum temperature (*Mean T*, *Max. T*, *Min. T*), monthly dewpoint temperature (T_D), and monthly minimum and maximum vapor pressure deficit (*Min. VPD*, *Max. VPD*).

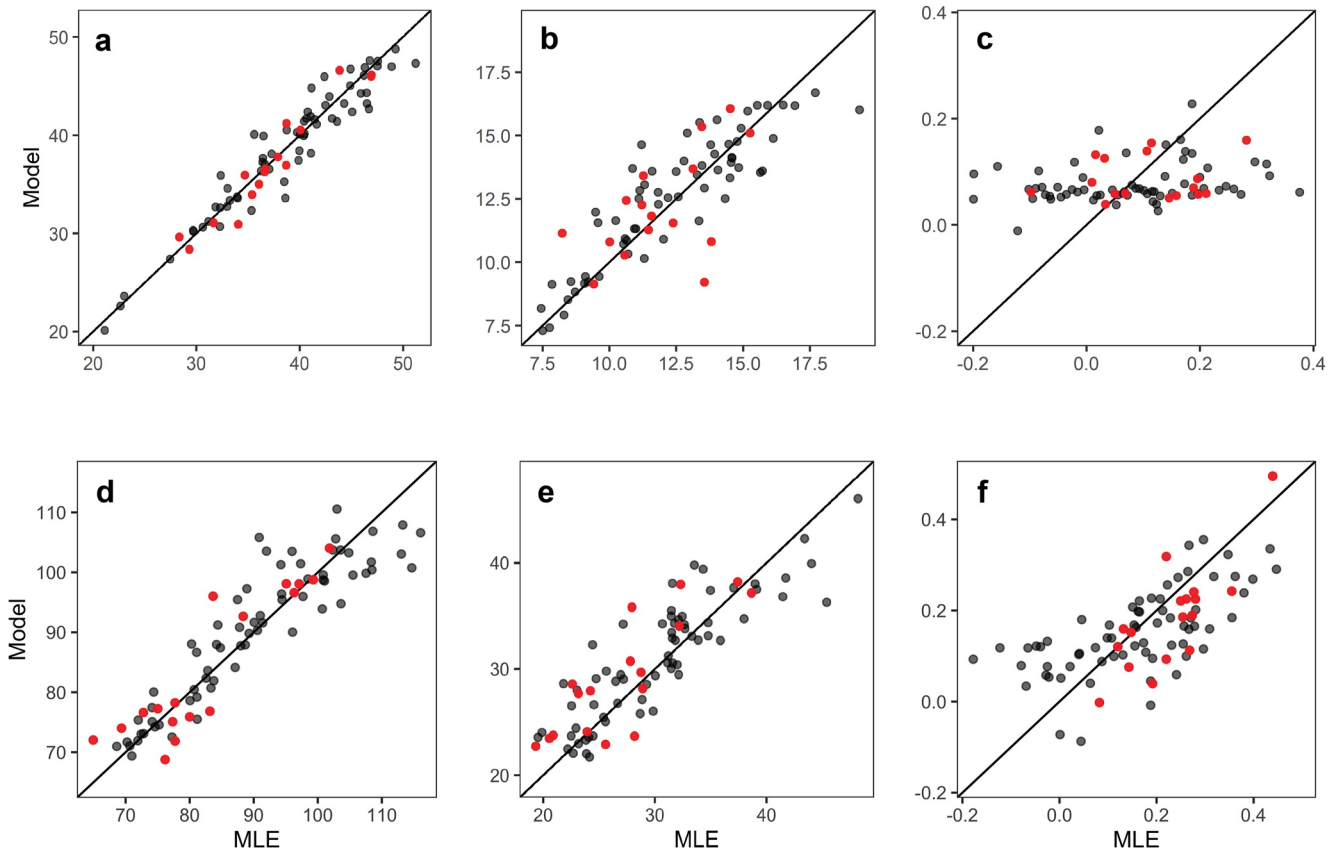

Figure 3. QQ-plots of the modeled trend surface versus maximum likelihood estimation (MLE) of the annual maxima data. Plots (a–c) are for the northeastern Colorado region's (a) location, (b) scale, and (c) shape, while plots (d–f) are for the Texas-Louisiana region's (d) location, (e) scale, and (f) shape. Black markers represent the calibration sites and red markers represent the validation sites.

the TXLA region. The best model out of those that used a fixed shape parameter ranked 333rd overall based on the TIC scores (Table S1 in Supporting Information S1).

The shape parameter results for the NECO region (Figure 3c) may indicate that either an extended set of covariates will not improve the estimates for every region or (more likely) that covariates beyond those selected here are needed for improved fits of the region's shape parameter. Although the NECO region's shape parameter fit can likely be improved further, we have achieved an improved fit over the standard fixed value that is used in practice. The NECO region's top 20 models (based on TIC) favored no more than three non-zero covariates for the shape parameter. However, the NECO model performance still benefited from the inclusion of these few covariates. The topmost model with a fixed shape parameter ranked 32nd based on its TIC score (Table S1 in Supporting Information S1).

Among the top 20 best performing models, only one of the annually averaged covariates (annual precipitation squared) appeared within the TXLA scale parameter's model. However, the first instance of its incorporation is the 12th ranked model for the region. Therefore, despite the differences between NECO and TXLA, the monthly covariates resulted in improved model performance for both regions and are worth exploring when building models for other regions.

5. Conclusions

Due to the spatial nature of extreme climate events, the estimation of exceedance probabilities for infrastructure design and hazard mitigation depends on properly modeling the spatially varying marginal parameters. In a block maxima approach, the selection of trend surfaces to properly capture the spatially varying generalized extreme value (GEV) marginal parameters can be non-trivial when a large set of relevant covariates are available.

Traditionally, latitude, longitude, and mean annual or seasonal precipitation are used to model the spatial variability of the GEV location and scale parameters, while the shape parameter is often set to a fixed value. We introduce elastic-net regularization as a simple and effective means to systematically identify optimal trend surfaces for the modeling of extreme events while exploring a larger set of physically relevant covariate information than is typical. We demonstrate the proposed method for modeling trend surfaces for extreme 24-hr duration precipitation using an extended set of geographic and climatological covariate information for two climatically distinct regions, northeastern Colorado (NECO) and the TXLA Gulf Coast. The 190 covariates explored for both regions were selected based on the rainfall-temperature thermodynamic relationship and the impact of physical information (e.g., elevation, climatology) on local extreme precipitation. We also demonstrate that there is a benefit to testing results beyond simply using the minimizing, or best regularizing, independently derived elastic-net results identified through k-fold cross-validation. The final trend surface results fit relatively well for both regions' GEV location and scale parameters. For the TXLA region, the method enabled the identification of useful covariates that allowed for an improved fit of the GEV shape parameter, which is often a difficult parameter to fit and is usually set to a fixed value. Our results indicate that setting the shape parameter to a fixed value greatly reduces the model performance for this region, as the topmost performing model that used a fixed shape parameter was ranked 333rd overall for the region. While the NECO region's shape parameter fit can still benefit from further improvement, the inclusion of covariates did improve model performance over models using a fixed shape parameter. The topmost model within the NECO region that used a fixed shape parameter was ranked 32nd overall. The results for both TXLA and NECO demonstrate that diverse regions may benefit from the exploration and addition of covariates. The NECO results also indicate that there are likely additional covariates that remain to be explored in future work, beyond the relatively extensive set used here, that may further improve the fit of the shape parameter. Additionally, we found that monthly covariates resulted in improved model performance for both regions relative to annual covariates, indicating that monthly covariates are worth exploring when constructing models for other regions. This simple effective approach for trend surface development is not specific to extreme precipitation analyses but can be applied to trend surfaces for other event types and can be implemented within various modeling approaches. Further, spatial trend surfaces and more reliable analysis of spatial extremes can also improve downscaling and disaggregation schemes (e.g., Papalexiou et al., 2018; Wilby & Wigley, 1997). Future related work will focus on more seamless automatic variable selection directed regularization approaches, for example, simultaneous rather than independent trend surface development.

Data Availability Statement

Figures, data analysis, and modeling where performed using R (R Core Team, 2020). R packages "glmnet" (Simon et al., 2011) and "SpatialExtremes" (Ribatet, 2020) were used for the elastic-net regularization and spatial GEV stages of the trend surface modeling, respectively. The covariate data employed is from the Parameter-elevation Relationships on Independent Slopes Model (PRISM) Norm81m long-term (1981–2010) (Daly et al., 2008) 30-year normals data set in 30 arc s resolution can be accessed at https://prism.oregonstate.edu/normals/. Note that since our retrieval of the PRISM Norm81m data set in October 2019, the PRISM Climate Group has updated the data set to Norm91m 30-year normals spanning the period of 1991–2020. Observed daily precipitation data was retrieved (downloaded 13 October 2019) from the NOAA Global Historical Climatology Network-Daily (GHCN-Daily) data set (Menne, Durre, Korzeniewski, et al., 2012; Menne, Durre, Vose, et al., 2012) for both study regions. Study region extents are based on the U. S. Geological Survey (USGS) Watershed Boundary Data set (WBD) for 2-digit Hydrologic Units 08, 10, and 12 (USGS, 2020a; USGS, 2020b, 2020c).

Acknowledgments
CAL was partially supported by USACE Contract Number W912HZ-16-A-0080, National Science Foundation Award No. CMMI-1635797, and National Oceanic and Atmospheric Administration Award No. NA19OAR4310294.

References

Adler, R. F., Gu, G., Wang, J.-J., Huffman, G. J., Curtis, S., & Bolvin, D. (2008). Relationships between global precipitation and surface temperature on interannual and longer timescales (1979–2006). *Journal of Geophysical Research*, *113*(D22), D22104. https://doi.org/10.1029/2008JD010536

Banerjee, S., Carlin, B. P., Gelfand, A. E., Carlin, B. P., & Gelfand, A. E. (2014). *Hierarchical modeling and analysis for spatial data*. Chapman and Hall/CRC. https://doi.org/10.1201/b17115

Blanchet, J., & Davison, A. C. (2011). Spatial modeling of extreme snow depth. *Annals of Applied Statistics*, *5*(3), 1699–1725. https://doi.org/10.1214/11-AOAS464

Coles, S. (2001). *An introduction to statistical modeling of extreme values*. Springer.

Coles, S., & Casson, E. (1998). Extreme value modelling of hurricane wind speeds. *Structural Safety*, *20*(3), 283–296. https://doi.org/10.1016/S0167-4730(98)00015-0

Cooley, D. (2009). Extreme value analysis and the study of climate change. *Climatic Change*, *97*(1–2), 77–83. https://doi.org/10.1007/s10584-009-9627-x

Cooley, D., Nychka, D., & Naveau, P. (2007). Bayesian spatial modeling of extreme precipitation return levels. *Journal of the American Statistical Association*, *102*(479), 824–840. https://doi.org/10.1198/016214506000000780

Daly, C., Halbleib, M., Smith, J. I., Gibson, W. P., Doggett, M. K., Taylor, G. H., et al. (2008). Physiographically sensitive mapping of climatological temperature and precipitation across the conterminous United States. *International Journal of Climatology*, *28*(15), 2031–2064. https://doi.org/10.1002/joc.1688

Davison, A. C., Padoan, S. A., & Ribatet, M. (2012). Statistical modeling of spatial extremes. *Statistical Science*, *27*(2), 161–186. https://doi.org/10.1214/11-STS376

Friedman, J., Hastie, T., & Tibshirani, R. (2010). Regularization paths for generalized linear models via coordinate descent. *Journal of Statistical Software*, *33*(1), 1–22. https://doi.org/10.18637/jss.v033.i01

Gumbel, E. J. (1958). *Statistics of extremes*. Columbia University Press. https://doi.org/10.7312/gumb92958

Hastie, T., Qian, J., & Tay, K. (2016). *An introduction to 'glmnet'*. Retrieved from https://glmnet.stanford.edu/articles/glmnet.html

Hastie, T., Tibshirani, S., & Friedman, H. (2009). *The elements of statistical learning: Data mining, inference, and prediction* (2nd ed.). Springer-Verlag.

Hoerl, A. E., & Kennard, R. W. (1970). Ridge regression: Biased estimation for nonorthogonal problems. *Technometrics*, *12*(1), 55–67. https://doi.org/10.2307/1267351

James, G., Witten, D., Hastie, T., & Tibshirani, R. (2013). *An introduction to statistical learning: With applications in R* (Vol. 112). Springer.

Javier, J. R. N., Smith, J. A., England, J., Baeck, M. L., Steiner, M., & Ntelekos, A. A. (2007). Climatology of extreme rainfall and flooding from orographic thunderstorm systems in the upper Arkansas River Basin. *Water Resources Research*, *43*(10). https://doi.org/10.1029/2006WR005093

Luke, A., Vrugt, J. A., AghaKouchak, A., Matthew, R., & Sanders, B. F. (2017). Predicting nonstationary flood frequencies: Evidence supports an updated stationarity thesis in the United States. *Water Resources Research*, *53*(7), 5469–5494. https://doi.org/10.1002/2016WR019676

Menne, M. J., Durre, I., Korzeniewski, B., McNeill, S., Thomas, K., Yin, X., et al. (2012). *Global historical climatology network-daily (GHCN-daily) version 3*. NOAA National Centers for Environmental Information. Retrieved from https://www.ncei.noaa.gov/metadata/geoportal/rest/metadata/item/gov.noaa.ncdc:C00861/html

Menne, M. J., Durre, I., Vose, R. S., Gleason, B. E., & Houston, T. G. (2012). An overview of the global historical climatology network-daily database. *Journal of Atmospheric and Oceanic Technology*, *29*(7), 897–910. https://doi.org/10.1175/JTECH-D-11-00103.1

Oki, T., Musiake, K., & Koike, T. (1991). Spatial rainfall distribution at a storm event in mountainous regions, estimated by orography and wind direction. *Water Resources Research*, *27*(3), 359–369. https://doi.org/10.1029/90WR02427

Papalexiou, S. M., Markonis, Y., Lombardo, F., AghaKouchak, A., & Foufoula-Georgiou, E. (2018). Precise temporal disaggregation preserving marginals and correlations (DIPMAC) for stationary and nonstationary processes. *Water Resources Research*, *54*(10), 7435–7458. https://doi.org/10.1029/2018WR022726

R Core Team. (2020). R: A language and environment for statistical computing [Computer software manual]. R Core Team. Retrieved from https://www.R-project.org/

Renard, B. (2011). A Bayesian hierarchical approach to regional frequency analysis. *Water Resources Research*, *7*(11), W11513. https://doi.org/10.1029/2010WR010089

Ribatet, M. (2009). *A user's guide to the spatialextremes package*.

Ribatet, M. (2017). Modelling spatial extremes using max-stable processes. In *Nonlinear and stochastic climate dynamics* (pp. 369–391). Cambridge University Press. https://doi.org/10.1017/9781316339251.014

Ribatet, M. (2020). SpatialExtremes: Modelling spatial extremes [Computer software manual]. R Package Version 2.0-9. Retrieved from https://CRAN.R-project.org/package=SpatialExtremes

Ribatet, M., Cooley, D., & Davison, A. C. (2012). Bayesian inference from composite likelihoods, with an application to spatial extremes. *Statistica Sinica*, *22*(2), 813–845.

Schumacher, R. S., & Johnson, R. H. (2006). Characteristics of U.S. extreme rain events during 1999–2003. *Weather and Forecasting*, *21*(1), 69–85. https://doi.org/10.1175/WAF900.1

Shepherd, J. M., Grundstein, A., & Mote, T. L. (2007). Quantifying the contribution of tropical cyclones to extreme rainfall along the coastal southeastern United States. *Geophysical Research Letters*, *34*(23). https://doi.org/10.1029/2007GL031694

Simon, N., Friedman, J., Hastie, T., & Tibshirani, R. (2011). Regularization paths for cox's proportional hazards model via coordinate descent. *Journal of Statistical Software*, *39*(5), 1–13. https://doi.org/10.18637/jss.v039.i05

Stedinger, J. R., & Griffis, V. W. (2008). Flood frequency analysis in the United States: Time to update. *Journal of Hydrologic Engineering*, *1313*(4), 1994–2204. https://doi.org/10.1061/(ASCE)1084-0699

Takeuchi, K. (1976). The distribution of information statistics and the criterion of goodness of fit of models. *Mathematical Science*, *153*, 12–18.

Tibshirani, R. (1996). Regression shrinkage and selection via the lasso. *Journal of the Royal Statistical Society: Series B*, *58*(1), 267–288. https://doi.org/10.1111/j.2517-6161.1996.tb02080.x

Tikhonov, A. N. (1943). On the stability of inverse problems. In *Doklady Akademii Nauk SSSR* (Vol. 39, pp. 195–198).

Trenberth, K. E., & Shea, D. J. (2005). Relationships between precipitation and surface temperature. *Geophysical Research Letters*, *32*(14). https://doi.org/10.1029/2005GL022760

USGS. (2020a). USGS watershed boundary dataset (WBD) for 2-digit hydrologic unit - 08 [Dataset]. U.S. Geological Survey (USGS). Retrieved from https://www.sciencebase.gov/catalog/item/5a1632b4e4b09fc93dd171e8

USGS. (2020b). USGS watershed boundary dataset (WBD) for 2-digit hydrologic unit - 10 [Dataset]. U.S. Geological Survey (USGS). Retrieved from https://www.sciencebase.gov/catalog/item/5a1632b6e4b09fc93dd171fb

USGS. (2020c). USGS watershed boundary dataset (WBD) for 2-digit hydrologic unit - 12 [Dataset]. U.S. Geological Survey (USGS). Retrieved from https://www.sciencebase.gov/catalog/item/5a1632b7e4b09fc93dd17202

Wikle, C. K., Berliner, L. M., & Cressie, N. (1998). Hierarchical Bayesian space-time models. *Environmental and Ecological Statistics*, *5*(2), 117–154. https://doi.org/10.1023/A:1009662704779

Wilby, R., & Wigley, T. (1997). Downscaling general circulation model output: A review of methods and limitations. *Progress in Physical Geography: Earth and Environment*, *21*(4), 530–548. https://doi.org/10.1177/030913339702100403

Zhao, W., & Khalil, M. a. K. (1993). The relationship between precipitation and temperature over the contiguous United States. *Journal of Climate*, *6*(6), 1232–1236. https://doi.org/10.1175/1520-0442(1993)006<1232:TRBPAT>2.0.CO;2

Zou, H., & Hastie, T. (2005). Regularization and variable selection via the elastic net. *Journal of the Royal Statistical Society: Series B*, *67*(2), 301–320. https://doi.org/10.1111/j.1467-9868.2005.00503.x